ISSN 0036-0295, Russian Metallurgy (Metally), Vol. 2019, No. 7, pp. 687–693. © Pleiades Publishing, Ltd., 2019.
Russian Text © The Author(s), 2019, published in Metally, 2019, No. 4, pp. 33–40.

Effect of Temperature on the Low-Cycle Fatigue Characteristics of Single Crystals Made of an Ni_3Al-Based Rhenium-Containing Intermetallic Alloy

K. B. Povarova[a, *], O. A. Bazyleva[b], M. A. Gorbovets[b], A. A. Drozdov[a, c], and M. A. Bulakhtina[a]

[a] *Baikov Institute of Metallurgy and Materials Science, Russian Academy of Sciences, Moscow, 119991 Russia*
[b] *All-Russia Research Institute of Aviation Materials, Moscow, 105005 Russia*
[c] *Bardin Central Research Institute for Ferrous Metallurgy, Moscow, 105005 Russia*
**e-mail: povarova@imet.ac.ru*

Received May 7, 2019; revised May 16, 2019; accepted May 24, 2019

Abstract—The low-cycle fatigue (LCF) of the single crystals made of a γ′-Ni_3Al-based VKNA-25 γ′ + γ nickel superalloy is studied at 10^4 cycles and a temperature of 20, 750, and 900°C. A temperature anomaly in the LCF fatigue limit of the VKNA alloy, namely, its increase with temperature in the range from 20 to 750°C, is detected. This anomaly is related to a change from octahedral to cubic slip at the temperature of the peak in $L1_2$-ordered alloys and to a change in the properties of the γ′ and γ phases. At normal temperature, the static tensile strength and the LCF characteristics of the [111] single crystals are higher than those of the single crystals with other crystallographic orientations (CGOs). The static tensile strengths of the [001] and [111] single crystals at 900°C and the strengths of the single crystals with all CGOs at 1000°C are almost the same, and the LCF fatigue limit of the [001] single crystals at 900°C is slightly higher than that of the [111] single crystals.

Keywords: nickel aluminide, cast single-crystal alloys, structure, strength, low-cycle fatigue, elevated temperatures, character of fracture

DOI: 10.1134/S0036029519070115

STATE AND FORMULATION OF THE PROBLEM

High-temperature structural γ′-Ni_3Al-based VKNA/(VIN) alloys have a lower density and a higher operating temperature [1, 2] than nickel superalloys [3–6]. Cast high-temperature and heat-resistant Ni_3Al-based alloys with low contents of refractory elements (W, Re, Mo) and surface-active metals (Ti, Zr, Hf, REM) consist of a γ′-Ni_3Al-based solid solution with an fcc $L1_2$-ordered crystal structure hardened by the precipitates of a nickel-based disordered fcc γ solid solution (ductile component). The main factor that provide the long life of heterophase γ′-Ni_3Al-based alloys is the high thermal stability of their structure–phase state due to the fact that these alloys are natural eutectic composites with the following contents of the main phases: 85–90 vol % γ′-Ni_3Al and 10–15 vol % γ-Ni [7].

The most strongly loaded parts, including gas turbine engine (GTE) blades, operate under thermal cycling, vibration, and cyclic alternating loads conditions, which induce diffusion and fatigue processes in materials. These processes degrade their structure and, hence, decrease the high-temperature strength, the ductility, and the fracture toughness of the materials. As a result, both operating temperature T_{op} and the service life of the most strongly loaded GTE parts are limited. Most fractures of modern GTE blades have a fatigue or thermal fatigue character. Although the fatigue strength is mainly determined by the design of a blade, the blade material also should have high resistance to fatigue crack propagation. The gradual damage accumulation under the action of repeated alternating cyclic stresses causes crack nucleation and growth and material fracture. The fracture can occur at the stresses that are much lower than the yield strength or the ultimate tensile strength, when fatigue damage or failure takes place during elastoplastic deformation [8, 9].

The data on the important characteristics of high-temperature structural alloys, such as the heat resistance and the low- (LCF) and high-cycle fatigue (HCF), of heterophase Ni_3Al-based alloys are scarce and random. Fermi energy, the authors of [10] were the first to study the crack nucleation and propagation along slip planes during a HCF investigation of a single-phase γ′-Ni_3Al single crystal. When studying HCF, the authors of [11] showed the important role of grain boundaries as the sites of crack nucleation in low-boron polycrystalline γ′-Ni_3Al. LCF tests were carried out on Ni_3Al single crystals to investigate the influence of cyclic stresses on the evolution of a dislocation substructure [12–15]. The investigation [16] of the influ-

Table 1. Average LCF fatigue limits of VKNA-25-type alloys with various CGOs during stress-controlled loading

T_{test}, °C	σ_{-1}, MPa, for CGO		
	⟨111⟩	⟨011⟩	⟨001⟩
20	860	660	740
750	840	740	840
900	620	580	660

ence of a crystallographic orientation (CGO) on the fatigue cracking of (100)[010] and (110)[110] single crystals made of a γ′-Ni_3Al alloy with 16.7 wt % Al, 8 wt % Cr, and 0.3 wt % B showed that crystallographic cracking could occur simultaneously on two or more slip planes in the {111} octahedron, which are tilted to the axis of a sample.

The data on the behavior of single-crystal heterophase γ′ + γ VKNA under low-cycle loading conditions are scarce and random. For example, the life of VKNA-25 alloy (with 0.015 wt % La) single crystals under LCF conditions at 10^4 cycles during stress–controlled loading of smooth specimens was studied in [17], and the behavior of VKNA-25 alloy single crystals at 850 and 1050°C during LCF tests under strain-controlled loading was investigated in [18]. The data on the orientation dependence of the LCF parameters in both works are conflicting. Obviously, it is necessary to comprehensively study the orientation dependence of the LCF characteristics of these alloys under various conditions in a wide temperature range.

The purpose of this work is to investigate the influence of temperature on the LCF characteristics of a cast single-crystal Ni_3Al-based VKNA-25 alloy with the main CGOs at 10^4 cycles during stress-controlled loading (repeated tension, stress ratio $R = 0.1$, loading frequency of 1 Hz) at temperatures up to 950°C.

EXPERIMENTAL

Experimental Materials and Techniques

The chemical composition of the VKNA-25 alloy is as follows (wt %): Ni base, 8.1–8.6 Al, 4.0–5.0 Co, 5.6–6.0 Cr, 4.5–5.0 Mo, 0.3–0.7 Ti, 1.2–1.6 Re, 2.5–3.5 W, 0.4 Si, 0.02 C, and 0.015 La. The impurity contents are as follows (wt %): 0.005 S, 0.005 P, 0.001 Pb, 0.0005 Bi, 0.003 Sn, and 0.003 Sb. The base composition was chosen so that the structure of a natural eutectic composite material containing 80–90 vol % γ′-Ni_3Al and 10–20 vol % γ-Ni that was thermally stable to near-melting temperatures formed in this alloy.

[001], [011], and [111] single crystals were grown by directional solidification (DS) with a temperature gradient $G = 150$ K/cm during solidification and a solidification rate $R = 10$ mm/min. For investigations, we chose single crystals with a deviation of ≤10° from a given CGO and the maximum block misorientation of 1°–2°. Samples were annealed at 1150°C for 1 h to remove casting and mechanical stresses. The microstructure of the samples was analyzed on an Olympus GX51 optical microscope and an LEO1420 scanning electron microscope. LCF tests at 10^4 cycles were performed during stress-controlled loading of smooth tensile fivefold proportional specimens (gage diameter of 5 mm) on a PSB-10 machine at temperatures of 20, 750, and 950°C. The LCF yield strength was determined as an average for 12 specimens. The mechanical properties of specimens with a length-to-diameter ratio of five were determined during static tension using standard techniques. The value per point for short-time tests was calculated as an average for at least three specimens.

RESULTS AND DISCUSSION

LCF Tests

Table 1 gives the average LCF yield strengths determined for each specimen batch at 10^4 cycles.

It should be noted that the LCF fatigue life of the VKNA-25 alloy at a temperature of 900°C and 10^4 cycles is close to that ZhS26-type nickel superalloys (660 ± 20 MPa) and has a lower density and a higher heat resistance than the nickel superalloys.

Character of Fracture

Figure 1 shows the appearance of some single crystals in the fracture zone at 20 and 900°C. Hereafter, we will use our results [2] of high-temperature LCF tests of the alloy under study at room temperature.

It should be noted that the deformation of all single crystals during LCF tests at 20°C occurs with multiple shear on {111} slip planes, which is indicated by the traces of intersection of these planes with the side specimen surfaces. These intersection traces are crack nucleation sources and are most pronounced in the [111] and [001] specimens (Figs. 1a, 1b). Predominant slip in a certain system of planes leads to the deformation of the gage portion of a specimen. As a result, the cross sections of the [111] and [001] specimens after LCF tests at 20°C become elliptical (see Figs. 1a, 1b). During LCF tests at 900°C, slip on planes is absent and the shape of the gage portion does not change. Before fracture, multiple cracks, which have rough edges and are perpendicular to the axis of applied stresses, form on the specimen surfaces (Fig. 1c). Traces of significant plastic deformation are visible in the fracture zones of the single crystals with all CGOs. The necking in the specimen tested at 750°C indicates concentrated deformation (Fig. 1d), and the reduction of the gage area in the specimen tested at 900°C points to predominant development of uniform deformation (Fig. 1e).

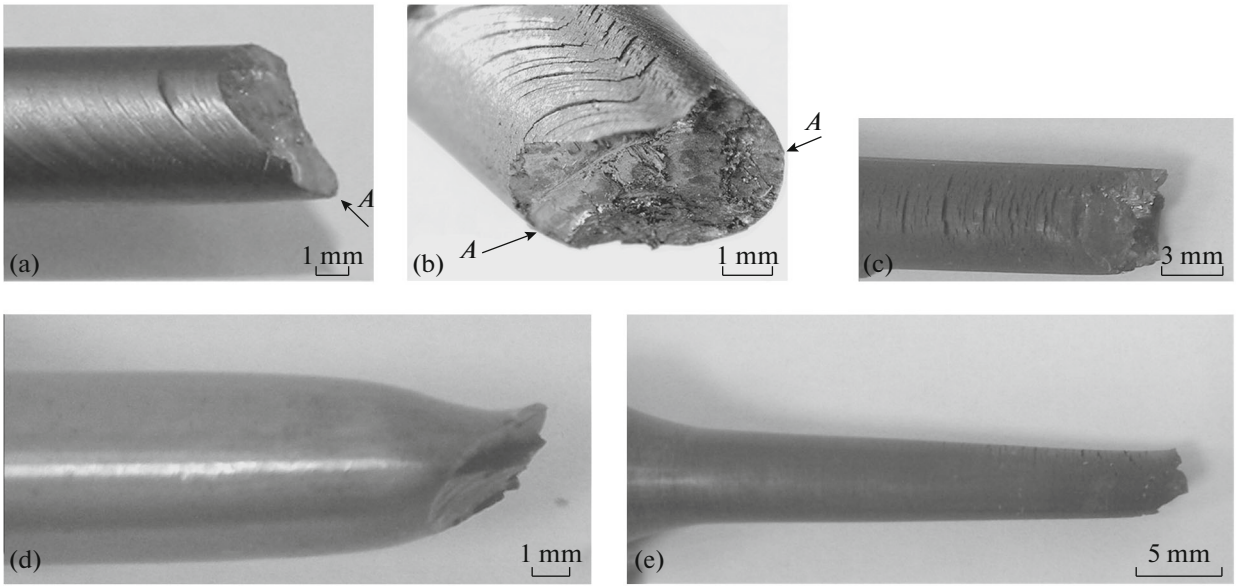

Fig. 1. Appearance of the single crystals with various CGOs in the fracture zone after LCF tests: (a) test at 20°C, ⟨111⟩ CGO; (b) 20°C, ⟨001⟩ CGO; (c) 900°C, ⟨001⟩; (d) 750°C, ⟨111⟩; and (e) 900°C, ⟨111⟩. Arrows *A* indicate crack nucleation sites.

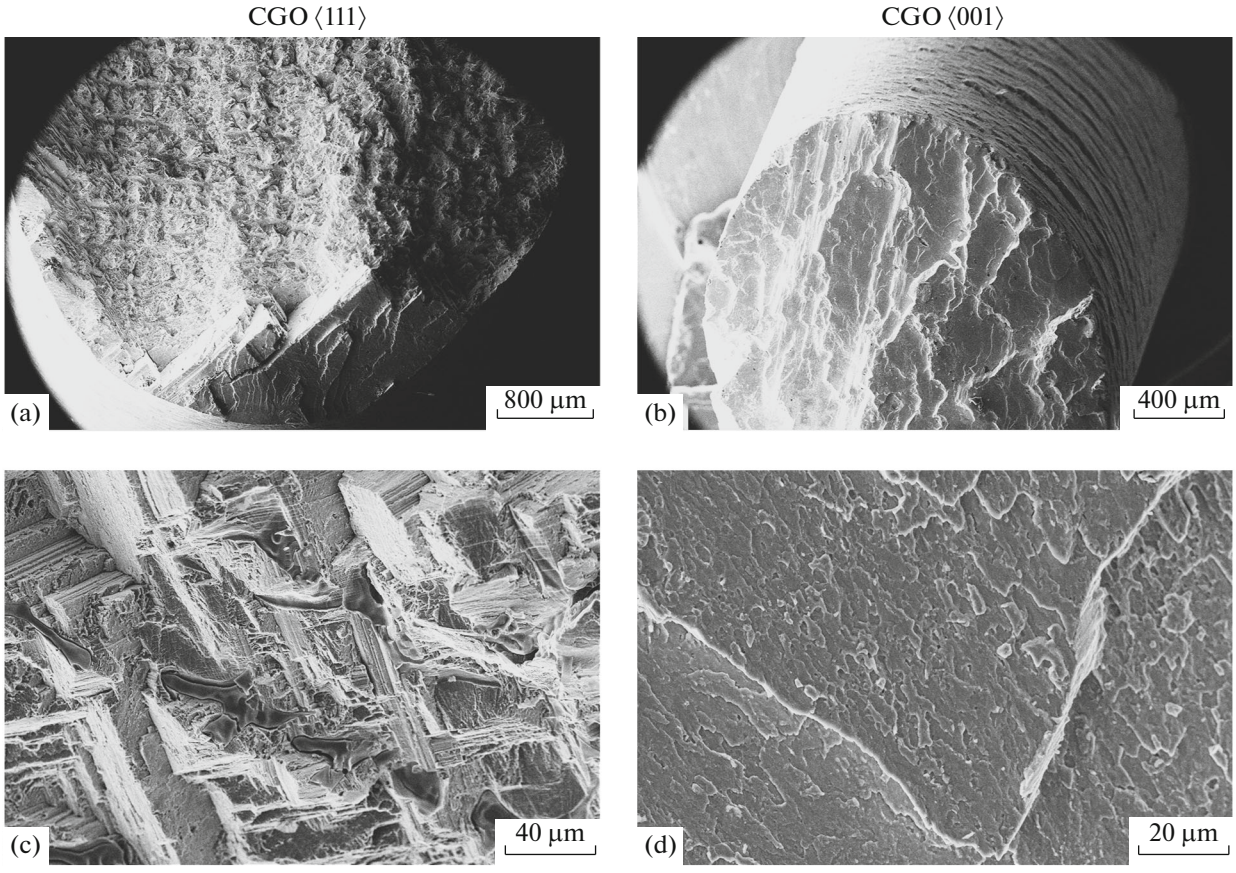

Fig. 2. Fracture surfaces of VKNA-25 alloy single crystals after LCF tests at (a, b) 20 and (c, d) 900°C.

The investigation of the fracture surfaces showed that the fracture of the single crystals with all CGOs was brittle and crystallographic at room temperature (Figs. 2a, 2b). The fracture at 900°C is preceded by significant plastic deformation, which is indicated by the formation of fracture ridges of different sizes on

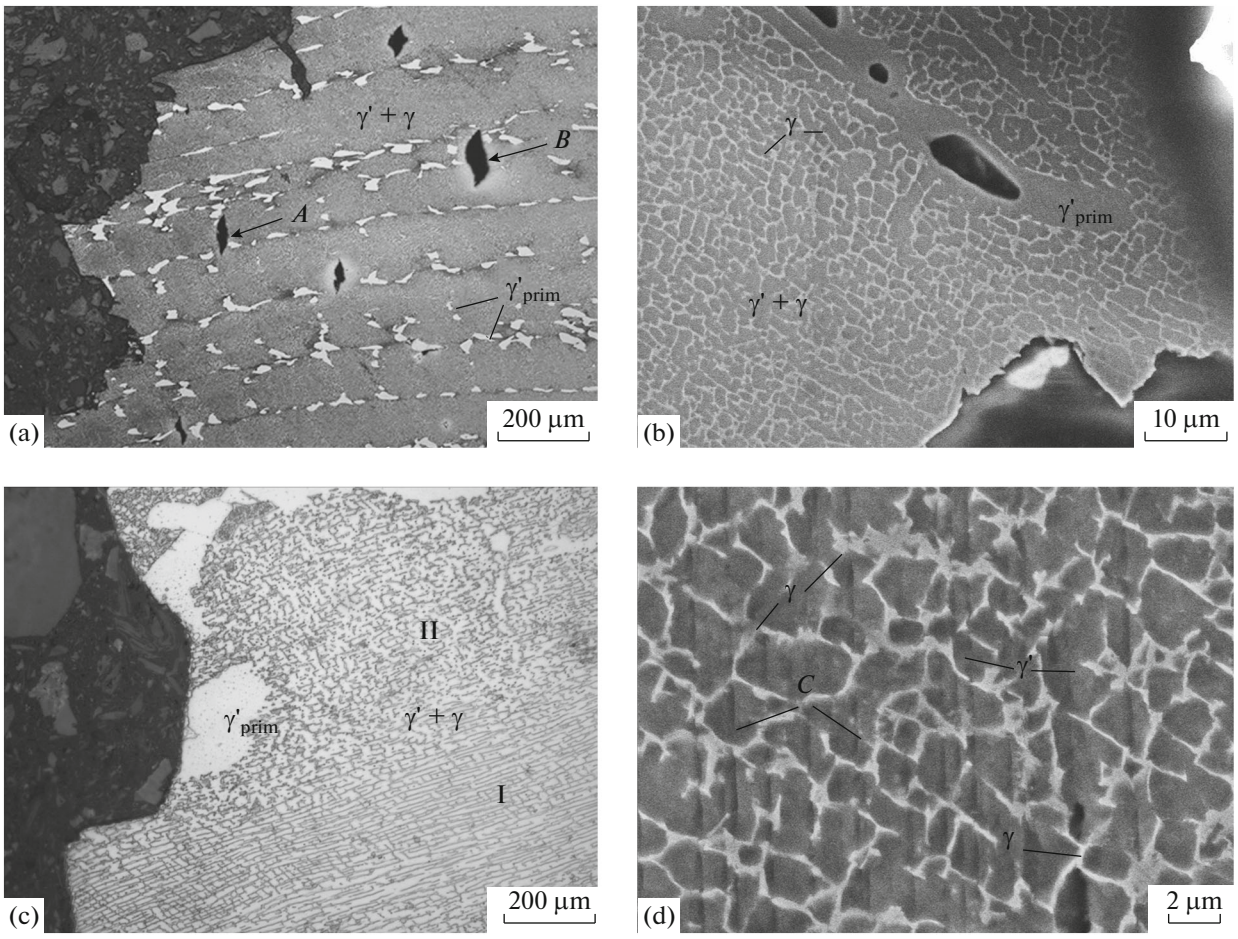

Fig. 3. Microstructure of the longitudinal section in the necks of the VKNA-25 alloy specimens failed during LCF tests at 900°C ((a, b) ⟨001⟩) and 20°C ((c, d) ⟨111⟩).

the fracture surface, and the traces of crystallographic fracture are weakly pronounced (Figs. 2c, 2d).

Microstructure

The DS single crystals have a dendritic–cellular structure [2]. Primary γ'-Ni_3Al (γ'_{prim}) precipitates are located in the interdendritic space of heterophase γ' + γ dendrites. The structure of the dendrites consists of γ'-phase regions separated by γ-phase layers (ductile structural constituent consists of a random fcc nickel-based solid solution). The fracture during LCF tests at 900°C is preceded by plastic macrodeformation. The neck of the specimen contains "fibers" formed by γ' + γ dendrites and rows of primary γ'-phase bent precipitates extended along the deformation direction (Fig. 3a). In the γ' + γ dendrites, the γ'-phase regions and the γ layers between them are elongated to form extended deformation bands with a raft structure (zone I), which alternate with the zones where γ'-phase regions are surrounded by discontinuous γ-phase layers (Fig. 3b, zone II).

During LCF tests at 900°C, transverse cracks appear both at the specimen surface and in the material volume (Fig. 1c). They can appear in dendrite arms (Fig. 3a, arrow *A*) and the interdendritic space (Fig. 3a, arrow *B*), and their appearance is not related to $\gamma'_{prim}/(\gamma' + \gamma)$ boundaries. Longitudinal cracks, which are characteristic of the fracture surfaces of the single crystals with all CGOs at 20°C (Fig. 3d, arrow *C*), are absent after tests at 900°C. At 750 and 900°C, a main crack paases across dendritic fibers normal to the axis of stresses and forms steps 2–3 dendrite high (see Fig. 3a).

No traces of macrodeformation are visible in the fracture zone after LCF tests at 20°C (Fig. 3c). The specimen retains the structure of the as-cast material: the γ'-phase regions separated by discontinuous γ-phase layers are equiaxed (see Figs. 3c, 3d).

It should be noted that the fractures of the γ' and γ phases in the two-phase region at 20°C are different: the γ' matrix undergoes brittle early fracture, and the γ layers are deformed by tension and are "pulled" from

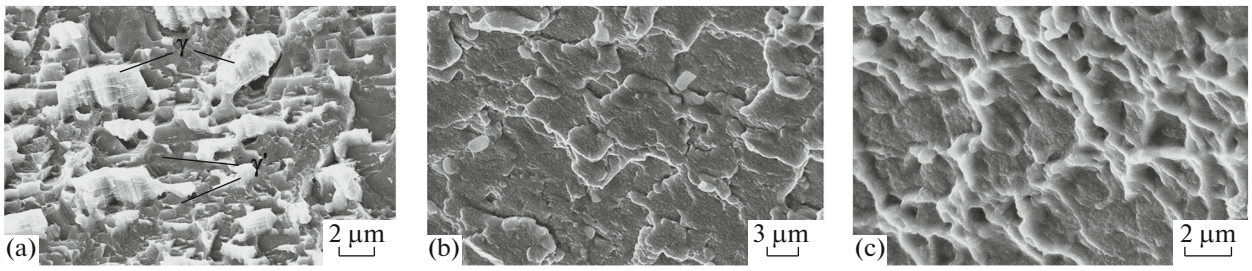

Fig. 4. Fracture surfaces of the ⟨111⟩ single crystal after LCF tests at 10^4 cycles and a temperature of (a) 20, (b) 750, and (c) 900°C.

the γ′-Ni_3Al_{eut} matrix in the tension direction to form "bridges" (Fig. 4a), which hinder the propagation of longitudinal cracks into the specimen volume (see Fig. 3d). In other words, the material was deformed as a composite material. After tests at 750 and 900°C, ductile fracture dimples occupy a high fraction on the fracture surfaces of the specimens, and the dimple sizes are 1–2 μm after tests at 750°C (Fig. 4b) and reach 7–15 μm after tests at 900°C (Fig. 4c).

Strength during Cyclic and Static Loading

Plastic strains is known to appear in the entire material volume under LCF test conditions, where the maximum cycle stresses exceed the elastic limit. The strains accumulate from cycle to cycle and reach the limiting value corresponding to material fracture during single static loading at a relatively small number of cycles. Therefore, it was interesting to compare the temperature dependences of fatigue limit σ^t_{LCF} during LCF stress-controlled loading tests at 10^4 cycles (Fig. 5a) and the ultimate tensile strengths of the VKNA-25 alloy single crystals with various CGOs (Fig. 5b).

As is seen from the curves, the changes in the fatigue limit during LCF tests (Fig. 5a) and the ultimate tensile strength of the VKNA-25 alloy single crystals with various CGOs (Fig. 5b) are nonmonotonic with increasing temperature. Both characteristics of the [001] and [011] single crystals exhibit strong temperature anomalies: when the test temperature increases from 20 to 750–850°C, the fatigue limit increases by 12–14% and the ultimate tensile strength increases by 48% for [001] CGO and by 68% for [011] CGO, and the LCF fatigue limit and the ultimate tensile strength decrease sharply only when the temperature increases to 900–1000°C. At all temperatures, the LCF fatigue limit of the [001] single crystals is higher than that of the [011] single crystals by 10–12%. As for the [111] single crystals, the LCF fatigue limit decreases weakly (by ~3%) when the temperature increases to 750°C, decreases sharply at 900°C, and occupies an intermediate position between the characteristics of the [001] and [011] single crystals. The ultimate tensile strength decreases more strongly (by ~34%), and the strengths of the single crystals with different CGOs at 1000°C are almost the same. Both characteristics of the [001] and [011] single crystals are characterized by an anomalous increase with a maximum in the temperature range 750–850°C.

DISCUSSION

The change in the character of fracture during LCF tests at 750 and 900°C as compared to LCF tests at 20°C and the anomalous increase in the LCF fatigue limit and the ultimate tensile strengths of the [001] and

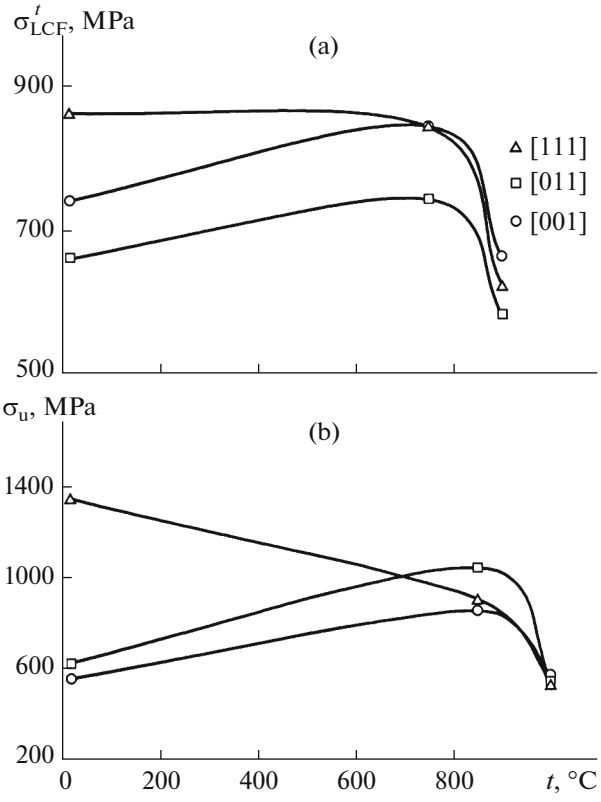

Fig. 5. Effect of temperature on (a) LCF fatigue limit σ^t_{LCF} during stress-controlled loading at 10^4 cycles and (b) ultimate tensile strengths of VKNA-25 alloy single crystals with various CGOs.

[011] single crystals (with a maximum in the temperature range 750–850°C) can be related to changes in slip systems during passage through the temperature of the yield and ultimate strength peak (near 800°C) and to the properties of the γ′ and γ phases (relative changes in their properties).

Change in Slip Systems

The substitution of cubic for octahedral slip was detected in many alloys with superstructures $L1_2$ (including Ni_3Al), $L1_0$ (TiAl), and some others when the temperature increases. Numerous studies of Ni_3Al-based IC-218, -221, -264, and -396 wrought alloys with a polycrystalline structure and cast VKNA alloys with a dendritic or single-crystal structure showed that the type of alloying can affect the peak height and shift the temperature of the maximum to certain limits and cannot affect the general character of the anomalous temperature dependence. The authors of [19] noted the following additional features of the deformation behavior of the intermetallic compound in the same temperature range: an anomalous temperature dependence of the strain-hardening coefficient of Ni_3Al and a weak dependence of the flow stress on strain rate $\dot{\varepsilon}$. The presence of blocked superdislocations in the range of the anomalous temperature dependence of the yield strength and the change from octahedral into cubic slip during passage through the temperature of the yield strength and ultimate strength peak accompany the nonmonotonic dependence of the deformation characteristics. It should be noted that changes in a deformation mechanism were detected in a single-crystal nickel superalloy. For example, the authors of [20] studied the changes in the dislocation structure during LCF tests of a γ + γ′ nickel superalloy and showed that, when temperature was increased from room temperature to 900°C, multiple slip changed gradually from planar at 20°C to wave slip at 750°C. When dislocations move in the γ matrix, they cut γ′-phase particles. An increase in the temperature to 900°C leads to cross sliding and dislocations pass by particles. Here, homogeneous deformation takes place; as a result, cracking induced by mode II fracture changes into mode I fracture.

Change in the Properties of the γ′ and γ Phases

The deformability of the γ′ and γ phases decreases with increasing temperature. As was shown in [17], the γ′ matrix undergoes early brittle fracture at room temperature, and the γ layers are deformed by tension and are pulled from the γ′-Ni_3Al_{eut} matrix in the tension direction. In other words, the material was deformed as a composite material. The plasticity characteristics of both phases at 750 and 900°C move toward each other because of an increase in the plasticity of the intermetallic compound. It should be noted that relative changes in the properties of the γ and γ′ phases with increasing temperature were also detected in a polycrystalline nickel superalloy containing 45 vol % γ′ phase. As was found by neutron diffraction in [21], the relative hardness of the two phases in a γ + γ′ superalloy changes gradually when the temperature increases: the γ′ phase is softer in the range between room temperature and 500°C, and the γ matrix is softer at higher temperatures (750°C).

Thus, despite some radical differences between the structures of γ′-Ni_3Al-based γ′ + γ alloys and γ + γ′ nickel superalloys, there are common features in changing a deformation mechanism and the character of their fracture during LCF tests in the temperature range 20–900°C.

CONCLUSIONS

(1) Under repeated tension conditions, we studied the LCF of single crystals made of a γ′-Ni_3Al-based VKNA-25 γ′ + γ superalloy at 10^4 cycles and temperatures of 20, 750, and 900°C. The detected temperature anomaly in the LCF fatigue limit of the VKNA alloy (increase with temperature from 20 to 750°C) is related to a change from octahedral to cubic slip at the temperature of the peak in $L1_2$-ordered alloys and to a change in the properties of the γ′ and γ phases.

(2) The LCF fatigue life of the VKNA-25 alloy at a temperature of 900°C and 10^4 cycles is close to that ZhS26-type nickel superalloys (660 ± 20 MPa) and has a lower density and a higher heat resistance than the nickel superalloys.

(3) The differences in the characters of fracture during LCF tests at 750–900 and 20°C are caused by an increase in the deformability of the γ′ phase with temperature: at 20°C, the material deforms as a composite material consisting of brittle γ′ and ductile γ components; at 750–900°C, the plasticity characteristics of the γ′ and γ phases move toward each other.

FUNDING

This work was supported by the Russian Foundation for Basic Research (project no. 19-03-00852/19) and was performed according to state assignment 075-00746-19-00.

REFERENCES

1. N. A. Nochovnaya, O. A. Bazyleva, D. E. Kablov, and P. V. Panin, *Intermetallic Alloys Based on Titanium and Nickel* (VIAM, Moscow, 2018).
2. K. B. Povarova, Yu. A. Bondarenko, A. A. Drozdov, O. A. Bazyleva, A. V. Antonova, A. E. Morozov, and E. G. Arginbaeva, "Effect of directional solidification on the structure and properties of Ni_3Al-based alloy single crystals alloyed with Cr, Mo, W, Ti, Co, Re, and REM," Russ. Metall., No. 1, 43–50 (2015).
3. R. C. Reed, *The Superalloys: Fundamentals and Applications* (Cambridge University Press, Cambridge, 2008).

4. S. M. Seo, J. H. Lee, Y. S. Yoo, Jo. H. Miyahara, and R. Ogi, "A comparative study of the γ/γ′ eutectic evolution during the solidification of Ni-base superalloys," Met. Mater. Trans. A **42**, 3150–3159 (2011).
5. H. T. Pang, H. B. Dong, R. Beanland, H. J. Stone, C. M. F. Rae, P. A. Midgley, G. Brewster, and N. D'Souza, "Microstructure and solidification sequence of the interdendritic region in a third generation single-crystal nickel-base superalloy," Met. Mater. Trans. A **40**, 1660–1669 (2009).
6. *Cast Gas-Turbine Engine Blades: Alloys, Technologies, Coatings*, Ed. by E. N. Kablov, 2nd ed. (Nauka, Moscow, 2006).
7. K. B. Povarova, "Physicochemical principles for designing thermally stable alloys based on the aluminides of transition metals," Materialovedenie, No. 12, 20–27 (2007); No. 1, 60–67 (2008).
8. V. S. Ivanova and V. F. Terent'ev, *Nature of the Fatigue of Metals* (Metallurgiya, Moscow, 1975).
9. V. F. Terent'ev, *Fatigue Strength of Metals and Alloys* (Intermet Inzhiniring, 2002).
10. J. E. Doherty, A. F. Giamei, and H. Rear, Met. Trans. A **6**, 2195– 2199 (1975).
11. N. S. Stoloff, G. E. Fuchs, A. K. Kuruvilla, and S. J. Choe, "Fatigue of intermetallic compounds," in *Proceedings of Conference on High Temperature Ordered Intermetallic Alloys II*, Ed. by N. S. Stoloff, C. Koch, C. T. Liu, and O. Izumi (Materials Research Society, Pittsburgh, 1987), Vol. 81, pp. 247–261.
12. N. R Bonda, D. P. Pope, and C. Laird, "Cyclic deformation of Ni_3(Al, Nb) single crystals at ambient and elevated temperatures," Acta Metallurgica **35**, 2371–2383 (1987).
13. N. R. Bonda, D. P. Pope, and C. Laird, "The dislocation structures of Ni_3(Al, Nb) single crystals fatigued at ambient and elevated temperatures," Acta Metallurgica **35**, 2385–2392 (1987).
14. L. M. Hsiung and N. S. Stoloff, "Mechanism of cyclic strain hardening in Ni_3Al + B single crystals," Acta Met. Mater. **40** (11), 2993–3000 (1992).
15. L. M. Hsiung and N. S. Stoloff, "Low-energy dislocation structures in cyclically deformed Ni_3Al single crystals," Acta Met. Mater. **42** (4), 1457–1467 (1994).
16. G. P. Zhang, Z. G. Wang, G. Y. Li, and S. D. Wu, "Crystallographic study of fatigue cracking in Ni_3Al (CrB) single crystal," Met. Mater. Trans. A **28**, 665 (1997).
17. K. B. Povarova, O. A. Bazyleva, A. A. Drozdov, N. A. Alad'ev, and M. A. Samsonova, "Low-cycle fatigue of an Ni_3Al-based VKNA-25 alloy at room temperature," Russian Metallurgy (Metally), No. 11, 880–891 (2012).
18. M. A. Gorbovets, O. A. Bazyleva, M. S. Belyaev, and I. A. Khodinev, "Low-cycle fatigue of a single-crystal VKNA intermetallic superalloy under conditions of "hard" loading," Metallurg, No. 8, 111–114 (2014).
19. B. A. Greenberg and M. A. Ivanov, *Intermetallic Compounds Ni_3Al and TiAl: Microstructure, Deformation Behavior* (Ural. Otd. Ross. Akad. Nauk, Yekaterinburg, 2002).
20. P. Li, Q. Q. Li, T. Jin, Y. Z. Zhou, J. G. Li, X. F. Sun, and Z. F. Zhang, "Comparison of low-cycle fatigue behaviors between two nickel-based single-crystal superalloys," Int. J. Fatigue **63**, 137–144 (2014).
21. M. R. Daymond, M. Preuss, and B. Clausen, "Evidence of variation in slip mode in a polycrystalline nickel-base superalloy with change in temperature from neutron diffraction strain measurements," Acta Mater. **55**, 3089–3102 (2007).

Translated by K. Shakhlevich